International Journal of Applied Science and Engineering
2006. 4, 2: 205-213

Development of Ultrasonic Clutch Module with Piezoelectric Vibrators

Kuo-Tsai Chang*

Department of Electrical Engineering,
National United University,
Miaoli 36003, Taiwan, R.O.C.

Abstract: This paper investigates the design, construction and performance test of an ultrasonic clutch module which includes two piezoelectric vibrators, two support frames, a preload control unit, a carbon brush unit and a base. For the vibrators, one vibrator acts as a driving frictional member connected to a driving motor, and the other vibrator acts as a driven frictional member connected to a driven load. In doing so, the design and construction of the clutch module are first expressed. Then, operating principle of the clutch module based on near-field acoustic levitation is expressed. Moreover, a test system, including the clutch module, the driving motor, the driven load and an AC power supply unit, is constructed to evaluate the performance of the clutch module. The AC power supply unit comprises two AC power supplies and two control switches. Finally, effects of electrical conditions on the performance of the clutch module are measured and discussed.

Keywords: ultrasonic clutch; frictional member; piezoelectric vibrator

1. Introduction

Mechanical frictional clutches such as overrunning clutches [1, 2], electrorheological (ER) clutches [3-6], disk clutches [7-10] and pneumatic clutches [11-13], have been applied to deliver a torque transmitted from a driving motor to an mechanical load using a frictional contact between the driving and driven frictional members for any type of mechanical frictional clutches. For an overrunning clutch as a one-way clutch, the one-way movement or torque transmission has been controlled by either the coupling of pawl and ratchet or the wedging of wedge and rolling pillar. The driving and driven members are mutually separated if the direction of the driving shaft is reverse, or the speed of the driving shaft is lower than that of the driven shaft. The structure of the overrunning clutch is simple. Unfortunately, the size of the overrunning clutch is vast, and the noise of that in separating state is high. For an ER clutch, a slight difference between driving and loading speeds and a great impact on the members are induced immediately after the facing surfaces of the members are coupled or separated. For a disk clutch, teeth and keys in each member are needed to link the facing surfaces of the members so as to finish the transmission of the torque. Both a large slip of the members and a great impact on each member are induced after coupling the facing surfaces. For a pneumatic clutch, an air bag is mounted in one of the members to govern the junction of the members. However, this clutch has many

* Corresponding author; e-mail: ktchang @ nuu.edu.tw
Accepted for Publication: May 5, 2006

unfavorable limitations, including large volume, large mass and high, production-cost, etc.

Next, conventional magnetic clutches such as permanent-magnet and magnetic-powder clutches have been used to govern the torque at the load side using magnetic coupling [14-18]. For a magnetic-powder clutch, strong magnetic links for delivering the torque from the motor to the load are induced in magnetic powders enclosed by a coil which is energized by a high magnetization current. Also, the loading torque is almost eliminated when the magnetization current is almost zero. The magnetic-powder clutch further exhibits an excellent performance in following respects: the speed control is stepless and the clutch is protected against overload. For a constant motoring torque, the loading torque increases with the magnetization current. A high magnetization current is needed to get a large torque transmitted from the driving motor to the load device, and to cause a strong electromagnetic interference (EMI). The EMI effect is extremely unfavorable in special environments such as hospitals, precision laboratories, etc. In order to mitigate or solve the aforementioned problems raised by the above conventional clutches, an ultrasonic clutch with piezoelectric elements such as piezoelectric buzzers, ultrasonic transducers or similar devices have been investigated and patented [19]. However, the ultrasonic clutch is not easily operated and constructed without a modular structure. To overcome the shortcomings, the present paper tends to provide a user-friendly modular ultrasonic clutch to govern a torque transmitted from a driving motor to a load device.

2. Materials and methods

2.1 Design and construction

From Figures 1a and 1b, the clutch module comprises two piezoelectric vibrators, two support frames, two connectors, a base, a preload control unit and a carbon brush unit. Each vibrator includes two adjoining piezoelectric ceramic disks, two non-adjoining cylindrical aluminum-alloy blocks, two electric rings and a bolt which is employed to clamp the ceramic disks and the aluminum-alloy blocks. The vibrator is a bolt-clamped Langevin piezoelectric vibrator (BLT-45282H, Increase-More Co. Ltd., Taipei, Taiwan) with inner diameter of 35 mm, outer diameter of 45 mm and length of 79.5 mm. All of the frames, connectors and base are composed of aluminum-alloy materials. The preload control unit consists of two bearings with 35 mm in outer diameter and 62 mm in inner diameter, an aluminum-alloy preload regulator with 30 mm in length, 62 mm in outer diameter and 30 mm in inner diameter and a wavelike steel disk spring with 7 mm in height, 60 mm in outer diameter and 47 mm in inner diameter which is mounted between one bearing and the preload regulator. The coefficient of elasticity for the disk spring is around 123 g/mm. Thus, a preload force on radiating surfaces of the vibrators is controlled by the preload regulator within the preload control unit.

From Figure 2, the carbon brush unit includes four carbon brush sets, a bakelite support and a metal base, where each carbon brush set consists of a carbon brush, a spirochete spring and a control screw. Then, the AC power is sent to the ceramic disks of each vibrator via two of the carbon brush sets and a sliding ring unit, as shown in Figure 3, attached on the vibrator. Here, the sliding ring unit comprises two copper rings and a plastic base, as depicted in Figure 4. In the construction of the clutch module, the bolt of the vibrator is first connected to the connector. Then, the small aluminum-ally block of the vibrator is inserted into the central hole of the bearing, and the bearing is further inserted into the central hole of the support frame at one side of the clutch module. Moreover, the disk spring is interposed between the bearing and the preload regulator which is partially screwed into the central hole of the support

frame. Furthermore, the clutch module is connected to a shaft of a driving motor using a flexible coupling, and connected to a shaft of a load device using another flexible coupling.

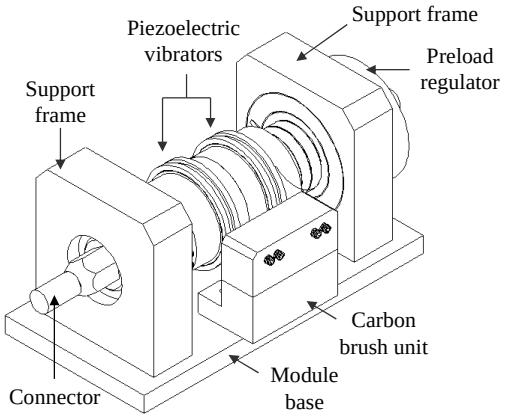

(a) Exploded diagram

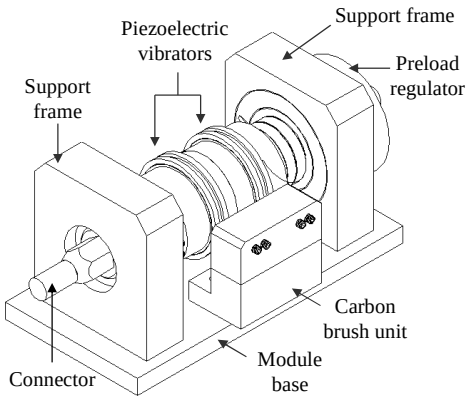

(b) Schematic diagram

Figure 1. Schematic diagrams of ultrasonic clutch module

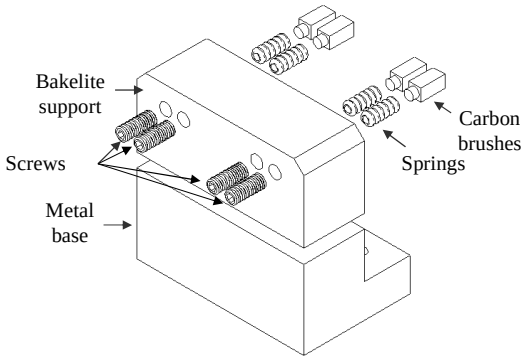

Figure 2. Assembly diagram of the carbon brush unit

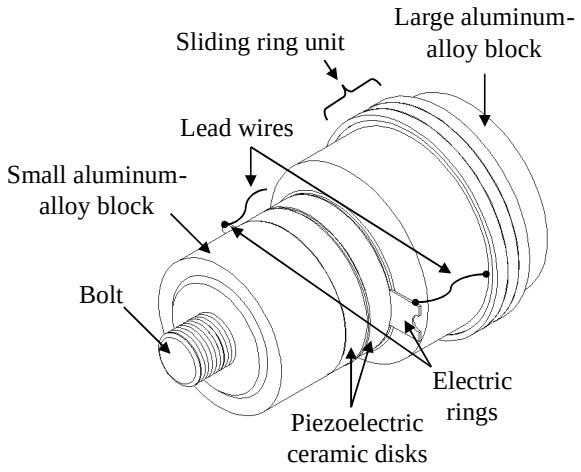

Figure 3. Structure of the piezoelectric vibrator sliding ring unitwith

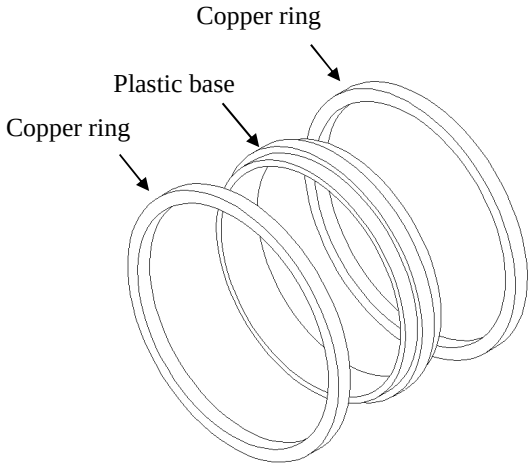

Figure 4. Exploder diagram of the sliding ring unit

2.2 Operating principles

Figure 5 reveals a schematic diagram of operating principle for performing the connection of the clutch module or getting a torque at the load device from the driving motor. From Figure 5, the radiation surfaces of the vibrators within the clutch module are coupled with each other to get a torque at the load device from the driving motor if neither vibrator is energized by AC power. Thus, the

radiation surfaces are separated from each other by near field acoustic levitation leading to loss of a torque transmitted from the driving motor to the load device if one of the vibrators is energized by a high AC power. Regarding the description of the acoustic levitation, as shown in Figure 6, an object with a planar-and-rigid bottom suspends above a radiation surface of a piezoelectric vibrator due to a radiation pressure Π (kgw/m^2) which is applied on the planar-and-rigid bottom. Meanwhile, many piston-like acoustic waves occur in the space between the planar-and-rigid bottom and the radiation surface.

When the wavelength λ of the acoustic wave greatly exceeds the levitation height h, i.e. λ [μm] >> h [μm], according to Chu *et al*. [20], the levitation height is given by

$$h \cong 0.5a_o \cdot \sqrt{(1+\gamma)\rho_a c_a^2 / \Pi} \qquad (1)$$

where ρ_a [kg/m^3]is the density of sound in the delivery medium, c_a [m/s] is the velocity of sound in the delivery medium, a_o [μm] is the amplitude of ultrasonic vibration on the radiation surface of the vibrator, and γ is the specific heating ratio. Here, the levitation height h is defined as a distance between the bottom of the object and the radiation surface of the vibrator. Using eq. (1), the levitation height increases with the vibration amplitude if the parameters such as ρ_a, c_a, Π and γ are constant. Also, the levitation height decreases as the radiation pressure increases if the parameters such as ρ_a, c_a, a_o and γ are constant. For special case, $h \cong a_o$ due to $\Pi=\Pi_{max}=0.5x[(1+\gamma)\rho_a c_a^2]^{1/2}$, where Π_{max} is the maximum radiation pressure. This finding indicates that crests of ultrasonic vibrations on the radiation surface of the vibrator are just contact with the bottom of the object.

2.3 Test system

From Figure 7, a test system, including the clutch module, a DC servomotor (U508T-012WL8, Sanyo Denki Co. Ltd., Taipei, Taiwan) and a magnetic clutch (OPC-10, Ogura Clutch Co. Ltd., Gunma, Japan), is constructed to evaluate the performance of the clutch module. The clutch module is mounted between the DC servomotor and the magnetic clutch which is acted as a mechanical load, and connected to shafts of the servomotor and the magnetic clutch using two flexible couplings (MFC-25, Ta Sun Good Enterprise Co. Ltd., Kaohsiung, Taiwan). All of the servomotor, the magnetic clutch and the clutch module are further fixed to a metal base using a lot of metal screws. A photograph of the test system is shown in Figure 8. Additionally, each of the motoring and loading speeds is detected by a digital optical tachometer (RM-1501, Prova Co. Ltd., Taipei, Taiwan) and eight optical reflectors which are uniformly attached on the flexible coupling near the servomotor or the magnetic clutch.

Next, the DC voltage V_M connected to the servomotor is controlled by a DC power supply (LPS-305, American Reliance Inc., California, USA), and the sinewave voltages, including v_{s1} and v_{s2}, connected to the vibrators within the clutch module are controlled by AC power supplies (1) and (2) shown in Figure 9. In Figure 9, the control switch SW1 or SW2 is employed to control the connection or disconnection between the sinewave voltage v_{s1} or v_{s2} and the associated vibrator. Each of the AC power supplies consists of a full-bridge switching resonant inverter, a driven and isolated circuit, a DC power supply (LPS-305, American Reliance Inc., California, USA) and a function generator (FG-506, American Reliance Inc., California, USA). Here, the inverter comprises a full-bridge switching DC chopper, a resonant tank and an equivalent circuit of the vibrator. In the control of the sinewave voltages, the amplitude of the sinewave v_{s1} or v_{s2} is controlled by the DC power supply, and the frequency of the sinewave voltage is controlled by the function generator.

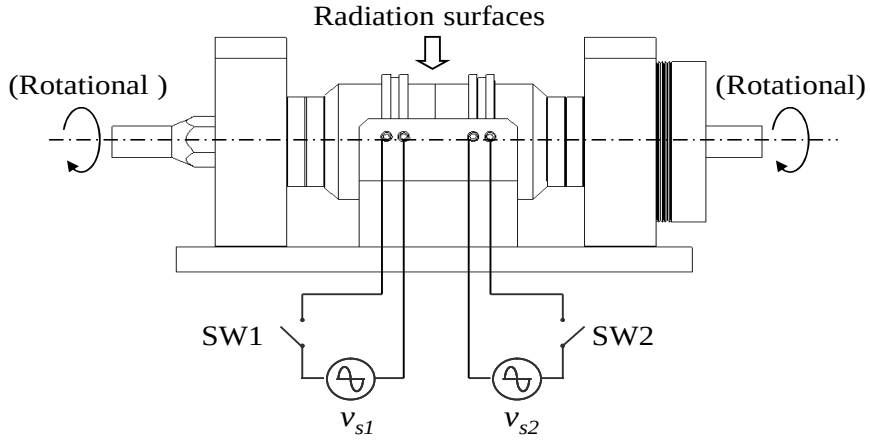

Figure 5. Operating principle of the ultrasonic clutch module

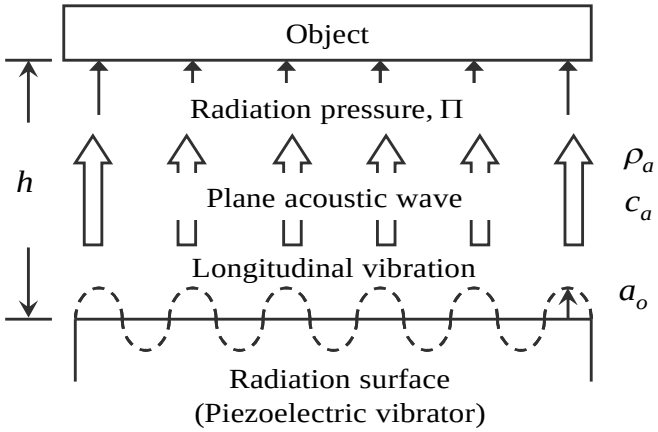

Figure 6. Schematic diagram of ultrasonic levitation

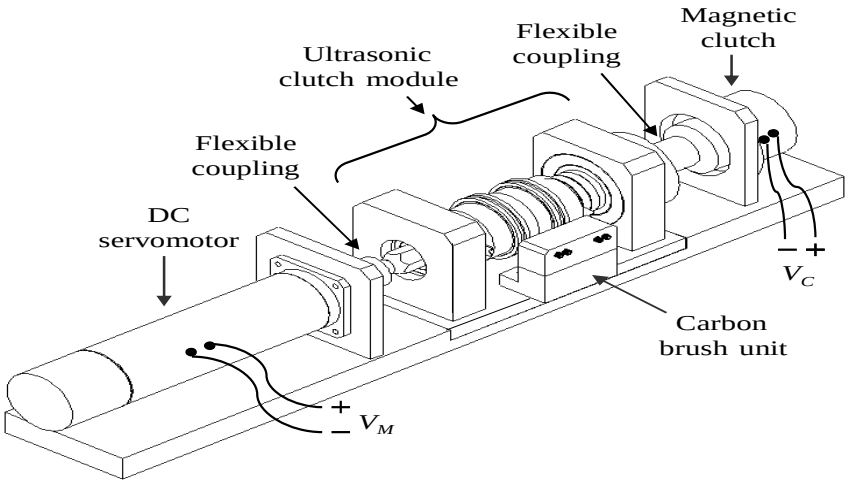

Figure 7. Schematic diagram of test system

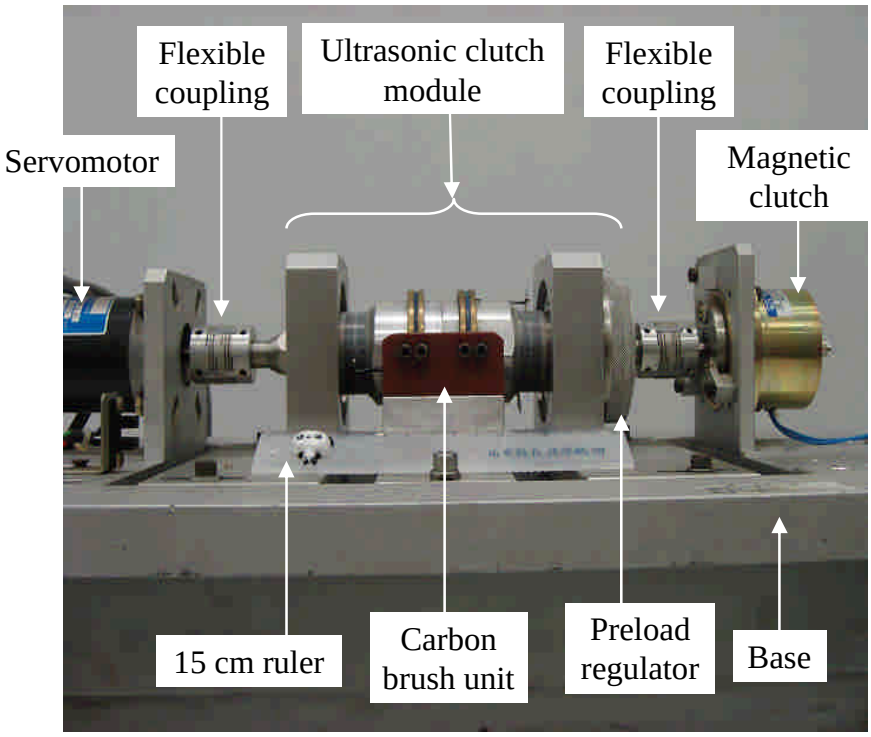

Figure 8. Photograph of test system

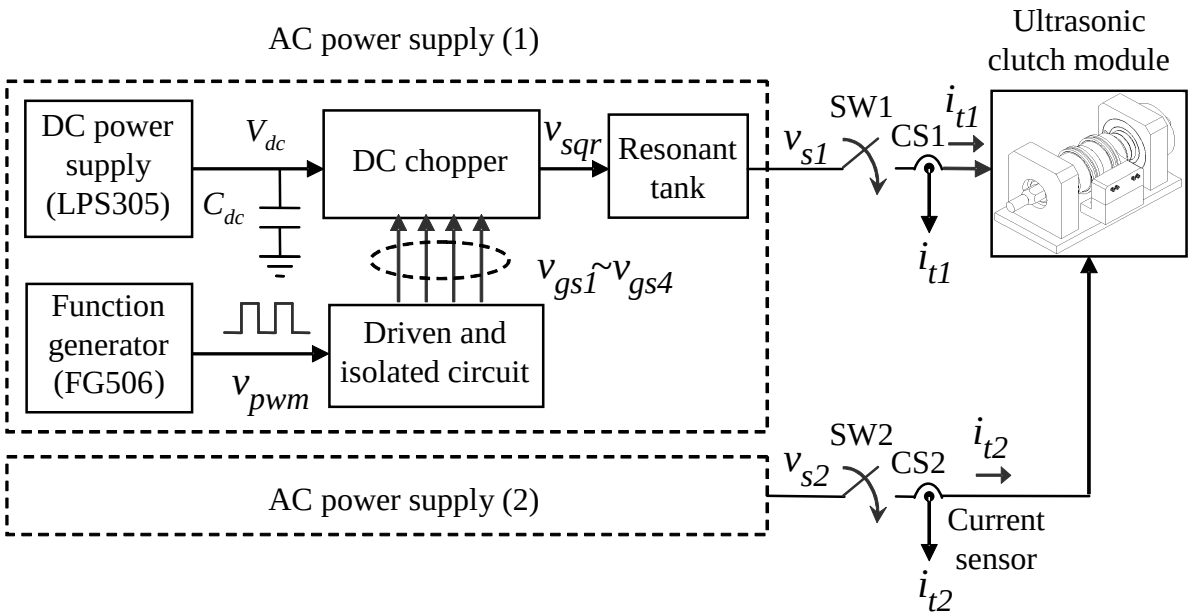

Figure 9. AC power supply system

3. Results and discussion

The preload force induced on the radiation surfaces of the vibrators within the clutch module is approximately 5 N. The motoring speed is approximately 600 rpm when the servomotor is energized by the DC voltage V_M (= 22 V). The magnetic clutch as a load device is not energized by the DC voltage V_C (= 0 V). From Figure 10, both of the motoring and loading speeds declines as the motional current of the vibrator increases. Hereon, the motional current almost equals the terminal current of the vibrator, and the resonance frequency of the vibrator declines as the amplitude of the sinewave voltage v_{s1} or v_{s2} at resonance. The results on the curve I are induced by one electrically energized vibrator, and those on the curve II are induced by two electrically energized vibrators. The loading speed almost equals the motoring speed (≅ 600 rpm) when only one of the vibrators is driven by a low motional current (≤ 0.2 A), or both of the vibrators are not energized by AC power. Also, the loading speed becomes a low speed such as 2.5 rpm when a high motional current (≥ 0.9 A) drives only one of the vibrators. The curve II reveals that a high motional current (≅ 0.98 A) markedly reduces the loading speed from 600 to 2.5 rpm. Additionally, the loading speed from the curve I slightly exceeds that from the curve II. Therefore, the clutch module is capable of governing the torque delivery from the servomotor to the load device through AC power control of the vibrators within the clutch module.

Next, a multi-function meter (YF-3140, Yu Hong Co. Ltd., Taichung, Taiwan) with an ohmmeter function, as shown in Figure 11, is connected to the large aluminum-alloy blocks of the vibrators within the clutch module using two probes to confirm the existence of the ultrasonic levitation which is induced in the space between the adjoining radiation surfaces of the vibrators. From the measured results, the resistance displayed on the display of the meter approximately equals infinity, and thus the ultrasonic levitation exists when both vibrators are driven by a high terminal current, i.e. $I_{t1} \cong I_{t2} \cong 0.98$ A. This resistance also almost equals zero, and thus the ultrasonic levitation vanishes when neither of vibrator is energized by AC power. For the electrical responses of the vibrator at resonance, according to Figure 12, the terminal current I_{t1} increases, and the resonance frequency f_r decreases when the driving voltage V_{s1} increases. In Figure 12, $I_{t1} \cong 0.42$ A and $f_r \cong 29.28$ kHz at $V_{s1} \cong 10$ V. Also, $I_{t1} \cong 0.98$ A and $f_r \cong 28.96$ at $V_{s1} \cong 80$ V.

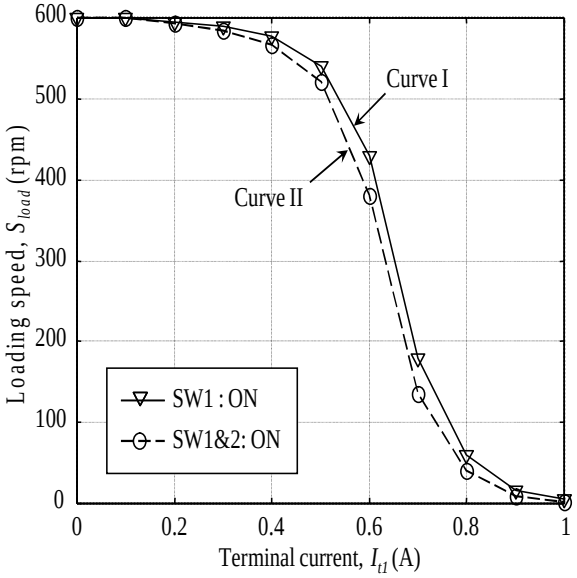

Figure 10. Relationship between loading speed and terminal current

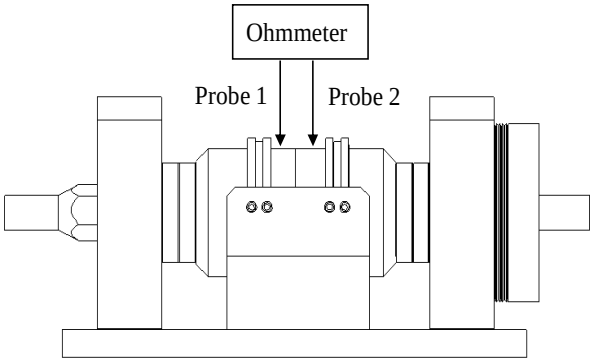

Figure 11. Experimental setup for verifying separation of the radiation surfaces

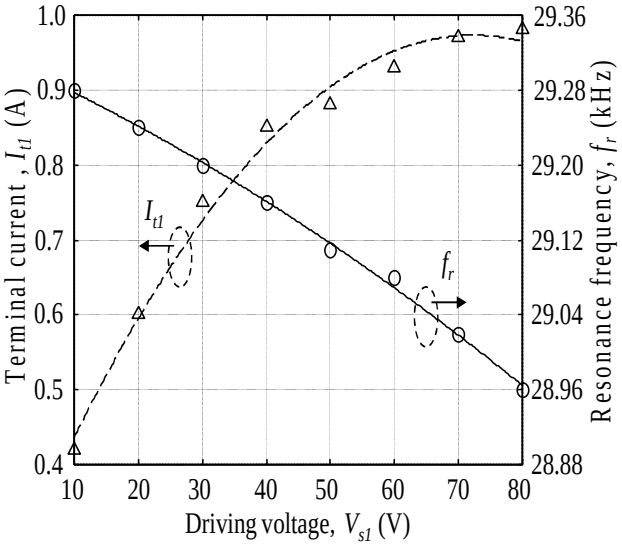

Figure12. Relationship between terminal current and resonance frequency

4. Conclusions

An ultrasonic clutch module is successfully mounted between a driving motor and a driven load for governing the connection or disconnection of torque delivery from the motor to the load. This module includes two piezoelectric vibrators, two support frames, a preload control unit, a carbon brush unit and a base. The clutch module is further connected to a shaft of the motor via a flexible coupling, and connected to a shaft of the load via another flexible coupling. Then, the radiation surfaces of the vibrators are forcibly coupled with each other, and thus the loading speed is equivalent to the motoring speed (≅ 600 rpm) when neither of vibrator is electrically energized by AC power. Also, the radiation surfaces are separated from each other, and thus the loading speed is approximately zero when only one of the vibrators is electrically energized by a high terminal current (≥ 0.9 A) under resonance operation. The motoring speed is still 600 rpm. Moreover, the loading speed decreases when the terminal current of the vibrator increases at resonance.

References

[1] Liu, K. and Bamba, E. 1998. Frictional dynamics of the overrunning clutch for pulse-continuously variable speed transmissions: rolling friction. *Wear*, 217: 208-214.

[2] Liu, K. and Bamba, E. 2005. Analytical model of sliding friction in an overrunning clutch. *Tribology International*, 38: 187-194.

[3] Tan, K. P., Stanway, R., and Bullough, W. A. 2006. Validation of dynamic torque response of an electrorheological (ER) clutch. *Mechanical System and Signal Processing*, 20: 463-492.

[4] Han, S.-S., Choi, S.-B., and Cheong, C.-C. 2000. Position control of X–Y table mechanism using electro-rheological clutches. *Mechanism and Machine Theory*, 35: 1563-1577.

[5] Monkman, G. J. 1997. Exploitation of compressive stress in electrorheological coupling. *Mechatronics*, 7: 27-36.

[6] Whittle, M., Atkin, R. J., and Bullough, W. A. 1995. Fluid dynamic limitations on the performance of an electrorheological clutch. *Journal of Non-Newtonian Fluid Mechanics*, 57: 61-81.

[7] Lee, J. M., Kim, B. M., and Kang, C. G. 2006. A study on the cold ironing process for the drum clutch with inner gear shapes. *International Journal of Machine Tools & Manufacture*, 46: 640-650.

[8] Afferrante, L., Ciavarella, M., Decuzzi, P., and Demelio, G. 2003. Transient analysis of frictionally excited thermoelastic instability in multi-disk clutches and brakes. *Wear*, 254: 136-146.

[9] Zagrodzki, P. and Truncone, S. A. 2003. Generation of hot spots in a wet multidisk clutch during short-term engagement, *Wear*, 254: 474-491.

[10] Afferrante, L. and Decuzzi, P. 2004. The effect of engagement laws on the thermomechanical damage of multidisk

clutches and brakes. *Wear*, 257: 66-72.

[11] Zhao, S., Wang, J, Wang, J, and He, Y. 2006. Expansion-chamber muffler for impulse noise of pneumatic frictional clutch and brake in mechanical presses. *Applied Acoustics*, 67: 580-594.

[12] Tanaka, H. and Wada, H. 1995. Electro-pneumatic clutch servomechanism and its fuzzy control for automated manual transmission. *JSAE*, 16: 212-217.

[13] Schulze, L. J. H, Congleton, J. J., Koppa, R. J., and Huchingson, R.D. 1995. Effects of pneumatic screwdrivers and workstations on inexperienced and experienced operator performance. *International Journal of Industrial Ergonomics*, 16: 175-189.

[14] Nagrial, M. H. 1993. Design optimization of magnetic couplings using high energy magnets. *Journal of Electric Machines and Power Systems*, 21: 115-126.

[15] Yonnet, J. P., Hemmerlin, S., Rulliere, E., and Lemarquand, G. 1993. Analytical calculation of permanent magnet couplings. *IEEE Transactions on Magnetics*, 29: 2932-2934.

[16] Albertz, D., Dappen, S., and Henneberger, G. 1997. Calculation of the induced currents and forces for a hybrid magnetic levitation system. *IEEE Transactions on Magnetics*, 33: 1263-1266.

[17] Charpentier, J. F. and Lemarquand, G. 1999. Optimal design of air-gap synchronous permanent magnet couplings. *IEEE Transactions on Magnetics*, 35: 1037-1046.

[18] Choi, C. and Park, K. 1999. Self-sensing magnetic levitation using a LC resonant circuit. *Sensors and Actuators-A*, 72: 169-177.

[19] Chang, K. T. and Ouyang, M.-S. 2005. Ultrasonic clutch. Patent No.: US6964327, USA.

[20] Chu, B. and Apfel, R. E. 1982. Acoustic radiation pressure produced by a beam of sound. *Journal of Acoustic Society American*, 72: 1673-1687.